Data reconciliation and optimal operation of a catalytic naphtha reformer

Tore Lid
Statoil Mongstad
5954 Mongstad

Sigurd Skogestad *
Department of Chemical Engineering
Norwegian Univ. of Science and Technology (NTNU)
Trondheim, Norway

December 18, 2006

*To whom all correspondence should be addressed (e-mail:skoge@chemeng.ntnu.no)

Abstract

The naphtha reforming process converts low-octane gasoline blending components to high-octane components for use in high-performance gasoline fuels. The reformer also has a important function as the producer of hydrogen to the refinery hydrotreaters. There are large seasonal variations in the reformer product price and two operational cases are studied. In case 1, the product price is high and throughput is maximized with respect to process and product quality constraints. In case 2, the product price is low and the throughput is minimized with respect to a low constraint on the hydrogen production. A process model based on a unit model structure, is used for estimation of the process condition using data reconciliation. Measurements are classified as redundant or nonredundant and the model variables are classified as observable, barely observable or unobservable. The computed uncertainty of the measured and unmeasured variables shows that even if a variable is observable it may have a very large uncertainty and thereby practically unobservable. The process condition at 21 data points, sampled from two years of operation, is estimated and operation is optimized. Based on the characteristics of the optimal operation a "self optimizing" control structure is suggested for each of the two operational cases.

1 Introduction

The naphtha reforming process converts low-octane gasoline blending components to high-octane components for use in high-performance gasoline fuels. "Octane" or, more precisely the octane number, is the measure or rating of the gasoline fuels antiknock properties. "Knocking" occurs in an engine when the fuel self detonates due to high pressure and temperature before it is ignited by the engine spark. Permanent damage of the engine cylinder and piston parts is a likely result of persistent "knocking". The most common measure of the octane number is the RON (Research Octane Number). By definition iso-octane (2,2,4 trimethyl pentane) is given an octane number (RON) of 100 and n-heptane an octane number of 0. A fuel with 95 RON has, by use of this measure, equal anti knock properties to a mixture of 95% of iso-octane and 5% n-heptane.

A simplified process model of a semiregenerative catalytic naphtha reformer, involving five pseudo components, was presented by Smith (1959) and validated against plant data. The same model was used in Bommannan et al. (1989), where reaction parameters where estimated from two sets of plant data, and in Lee et al. (1997) where a process with continuous catalyst regeneration was modeled. In all three cases above, good agreement with plant data where reported. These models are used for simulation and design purposes except in Taskar and Riggs (1997) where optimal operation during a catalyst cycle, is considered. Taskar and Riggs (1997) developed a more detailed model of a semiregenerative catalytic naphtha reformer, involving 35 pseudo components. They claimed that the simplified model is a oversimplification of the process but no details of the practical consequences of the discrepancies where presented.

In this paper the simplified model of Smith (1959) is used for modeling a catalytic naphtha reformer with continuous catalyst regeneration. The model uses the unit model structure of Lid and Skogestad (2006). Scaling is applied to the process model variables and equations to improve its numerical properties. The process model is compared to 21 data sets from the naphtha reformer at the Statoil Mongstad refinery. These data where collected in a two year period and includes feed and product analysis and process measurements. The current state of the process is estimated using data reconciliation (Tjoa and Biegler, 1991), where redundancy of measurements, observability of variables and uncertainty of the estimate are examined. The same model is also used for computation of optimal operation and economical analysis of two optimal operation. Based on this analysis, a model predictive control (MPC) structure for "optimal" operation of the process is suggested.

2 Data reconciliation

Data reconciliation is used to estimate the actual condition of the process and is obtained as the solution of

$$\begin{aligned} \min_{z} \quad & J(z) \\ \text{s.t.} \quad & f(z) = 0 \\ & A_r z = b_r \\ & z_{r\,\min} \leq z \leq z_{r\,\max} \end{aligned} \tag{1}$$

where $J = (y_m - Uz)^{\mathrm{T}} Q (y_m - Uz)$. All n_y measurements are collected in the measurement vector y_m. The matrix U gives a mapping of the variables z into the measurements where Uz represents the estimated value of the measurements y. The matrix U has n_y rows and in each row one nonzero value, equal to one, in element $U(i, j)$ where variable j correspond to measurement i in the measurement vector y.

The weighting matrix Q is set equal to the inverse of the measurement error covariance matrix Σ_m. The measurement error is in this case assumed to be normal distributed ($\mathcal{N}(\mu, \sigma)$) with zero mean $\mu = 0$ and variance σ^2. If the measurement errors are uncorrelated Σ_m is diagonal with the variance of measurement i along the diagonal ($\Sigma_m(i, i) = \sigma(i)^2$). In this case Q is a diagonal matrix where $Q(i, i) = 1/\sigma(i)^2$. The solution of problem 1, using the objective $J = (y - Uz)^{\mathrm{T}} Q (y - Uz)$, gives the maximum likelihood estimate of the process variables.

Real process data is expected to have measurements with gross errors. In this case the mean value of the measurement error $\mu \neq 0$. This will result in a biased estimate using the objective described above. In order to reduce this effect a distribution describing the likelihood of a gross error in a measurement is selected. The bivariate distribution from Tjoa and Biegler (1991) has a frequency function of measurement number i is written as

$$\varphi_i = \frac{1}{\sigma_i \sqrt{2\pi}} \left[(1-p) \exp\left(-\frac{1}{2} \frac{(y_i - U_i z)^2}{\sigma_i^2} \right) + \frac{p}{b} \exp\left(-\frac{1}{2} \frac{(y_i - U_i z)^2}{\sigma_i^2 b^2} \right) \right] \tag{2}$$

where U_i is row number i of the measurement matrix U. The probability of a gross error in a measurement $p < 0.5$ and the ratio of the standard deviation of a gross error to that of a random error $b > 1$.

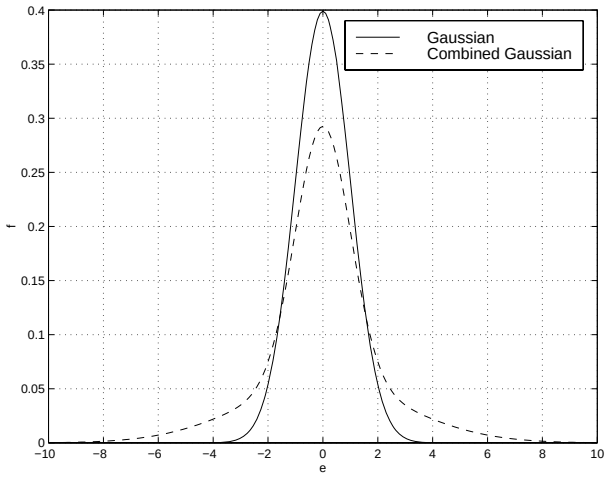

Figure 1: Gassian and combined Gaussian frequency function. The standard deviation $\sigma = 1$, probability for an outlier $p = 0.4$ and ratio of the standard deviations $b = 3$.

In figure 1 we can see that the probability of a measurement error in the range of $2 - 8 \times \sigma$ has increased. This makes the objective less sensitive to large errors. We define ψ as the log reciprocal of the error likelihood (φ_i) for each measurement and for a set of n_y measurements the objective function

$$J = -\sum_{i=1}^{n_y} \ln \left[(1-p) \exp\left(-\frac{1}{2} \frac{(y_i - U_i z)^2}{\sigma_i^2} \right) + \frac{p}{b} \exp\left(-\frac{1}{2} \frac{(y_i - U_i z)^2}{\sigma_i^2 b^2} \right) \right] \tag{3}$$

is minimized subject to process constraints.

A measurement is defined to have to have a gross error if the probability of the measurement error in the gross error distribution is larger than the probability of the random error distribution Tjoa and Biegler (1991). According to this definition a measurement has a gross error if

$$|y_i - U_i z| > \sigma_i \sqrt{\frac{2b^2}{b^2 - 1} \ln \left[\frac{b(1-p)}{p} \right]} \tag{4}$$

2.1 Observability and redundancy

Observability for unmeasured variables can be verified using the first order local observability sufficient condition from Stanley and Mah (1981). If

$$\text{rank} \begin{bmatrix} H_r(z^*) \\ U \end{bmatrix} = n_z \tag{5}$$

then the system is locally observable close to z^*. The linearized model equations $H_r(z^*)r$ are defined as

$$H_r(z^*) = \begin{bmatrix} \mathbb{F}(z^*) \\ Ar \end{bmatrix} \tag{6}$$

and U is the measurement matrix, $y = Uz$. A requirement is that the process model constraints should be continuously differentiable close to z^*

Redundancy for a measured value can be verified by removal of the row, corresponding actual measurement in U, making a new measurement mapping matrix U_{n_y-1}.

$$\text{rank} \begin{bmatrix} H_r(z^*) \\ U_{n_y-1} \end{bmatrix} = n_z \tag{7}$$

If the removed measurement is redundant then the rank of the matrix in equation 7 still has rank equal the total number of variables n_z.

2.2 Uncertainty of estimates

The uncertainty of a measured value is assumed to be normal distributed with zero mean and standard deviation σ. In order to give a indication of what is ideally gained using data reconciliation, the uncertainty of the reconciled variable is calculated.

The calculation of the error in the estimate is outlined as follows. The data reconciliation problem is linearized around the solution z_o with the measured values y_m. Then, variables in z are separated into measured variables y, unmeasured variables x and known or specified variables v. The specified and unmeasured variables are then removed from the problem. The data reconciliation problem is rewritten as a QP (quadratic programming) problem containing only the measured variables y and linear equality constraints. The QP problem has a known solution which can be written as $y = Gy_m$. The covariance of the measured values Σ_m is assumed to be known and the

uncertainty of the estimate is computed, using the propagation of error rule, which in the linear case gives $\Sigma_y = G\Sigma_m G^{\mathrm{T}}$.

The linearized data reconciliation problem from equation 1 is written as

$$\begin{aligned} \min_{z} \ & (y_m - U\tilde{z} - Uz_0)^{\mathrm{T}} Q (y_m - U\tilde{z} - Uz_0) \\ \text{s.t.} \quad & \left.\frac{\partial f(z)}{\partial z}\right|_{z=z_0} \tilde{z} + f(z_0) = 0 \\ & A_{r1}\tilde{z} = b_{r1} - A_{r1}z_0 \\ & A_{r2}\tilde{z} = b_{r2} - A_{r2}z_0 \end{aligned} \tag{8}$$

where $\tilde{z} = z - z_0$. The linear constraints are separated into two sets of linear constraints where A_{r1} and b_{r1} is the rows in A_r corresponding to the reactor equal efficiency constraints (according to equation 39). A_{r2} and b_{r2} is the constraints added to specify the values of known or specified values.

Using that $f(z_0) = 0$ and $A_{r1}z_0 = b_{r1}$ and $A_{r2}z_0 = b_{r2}$ the linearized data reconciliation problem is rewritten

$$\begin{aligned} \min_{z} \ & (y_m - U\tilde{z} - Uz_0)^{\mathrm{T}} Q (y_m - U\tilde{z} - Uz_0) \\ \text{s.t.} \quad & H\tilde{z} = 0 \\ & A_{r2}\tilde{z} = 0 \end{aligned} \tag{9}$$

where

$$H = \begin{bmatrix} \left.\frac{\partial f(z)}{\partial z}\right|_{z=z_0} \\ A_{r1} \end{bmatrix} \tag{10}$$

Now, the variables in $\tilde{z}$ are separated into measured variables $\tilde{y}$, unmeasured variables $\tilde{x}$ and specified variables $\tilde{v}$. Using that $y = Uz$ the data reconciliation problem is written

$$\begin{aligned} \min_{z} \ & (y_m - \tilde{y} - \tilde{y_0})^{\mathrm{T}} Q (y_m - \tilde{y} - \tilde{y_0}) \\ \text{s.t.} \quad & H_1\tilde{y} + H_2\tilde{x} + H_3\tilde{v} = 0 \\ & \widetilde{A}_{r2}\tilde{v} = 0 \end{aligned} \tag{11}$$

where H_1 is the columns of H corresponding to the measured values, H_2 is the columns of H corresponding to the unmeasured values and H_3 is the columns of H corresponding to the specified values. $\widetilde{A}_{r2}$ is the columns of A_{r2} corresponding to the specified values

The matrix $\widetilde{A}_{r2}$ has full rank and the specifications $\widetilde{A}_{r2}\tilde{v} = 0$ gives the solution $\tilde{v} = 0$.

Using that $\tilde{v} = 0$ and pre multiplying the linearized model equations $H_1\tilde{y} + H_2\tilde{x} + H_3\tilde{v}$ with a matrix P, defined such that $H_2^{\mathrm{T}}P = 0$, the unmeasured and specified variables are removed from the linear equality constraints. The resulting QP problem with linear equality constraints is written as

$$\begin{aligned} \min_{z} \ & (y_m - \tilde{y} - \tilde{y_0})^{\mathrm{T}} Q (y_m - \tilde{y} - \tilde{y_0}) \\ \text{s.t.} \quad & P^{\mathrm{T}} H_1 \tilde{y} = 0 \end{aligned} \tag{12}$$

Expanding the objective function, removing terms with fixed value, and multiplying by $\frac{1}{2}$ gives

$$J = \frac{1}{2}\tilde{y}^{\mathrm{T}} Q \tilde{y} + (y_0 - y_m) Q \tilde{y} \tag{13}$$

using the known solution of a QP problem with linear equality constraints the solution of equation 12 is written as

$$\tilde{y} = -Q^{-1}\left[I - A^{\mathrm{T}}(AQ^{-1}A^{\mathrm{T}})^{-1}AQ^{-1}\right] Q(y_o - y_m) \tag{14}$$

where $A = P^{\mathrm{T}}H_1$. Applying the propagation of error rule and substituting $Q = \Sigma_m^{-1}$ the covariance matrix if the estimation error Σ_y is computed as

$$\Sigma_y = \Sigma_m - \Sigma_m A^{\mathrm{T}}(A\Sigma A^{\mathrm{T}})^{-1} A\Sigma_m \tag{15}$$

When the measured values are known, values of the unmeasured variables are

$$\tilde{x} = (A_2^{\mathrm{T}}A_2)^{-1}A_2^{\mathrm{T}}A_1\tilde{y} \tag{16}$$

and similarly the covariance matric of the estimation error

$$\Sigma_x = (A_2^{\mathrm{T}}A_2)^{-1}A_2^{\mathrm{T}}A_1\Sigma_y A_1^{\mathrm{T}}A_2(A_2^{\mathrm{T}}A_2)^{-1} \tag{17}$$

3 Scaling

The process model $f(z) = 0$ is scaled according to the scaling procedure proposed in Lid and Skogestad (2006).

First, every equation is paired with one variable. The equation-variable pairing may be regarded as "equation i is used for computation of the value of variable j". It is written in a matrix P, where $P(i,j) = 1$ if variable j is paired with equation number i. All other values equals zero. This is done both for the linear specifications A_s and the nonlinear process model $f(z)$.

Second, all variables z are scaled $z = S_v * \bar{z}$ such that the scaled variable $\bar{z}$ has a value close to one. S_v is a $n_z \times n_z$ fixed diagonal variable scaling matrix.

Finally, the equation scaling matrices of the process model and the linear constraints, S_f and S_l, is computed as

$$S_{nl} = \left| \left[I \times \left(\frac{\partial f_i(z)}{\partial z} S_v P_{nl}^{\mathrm{T}} \right) \right]^{-1} \right| \tag{18}$$

$$S_l = \left| [I \times (A_s S_v P_l^{\mathrm{T}})]^{-1} \right| \tag{19}$$

where $\times$ denotes element by element multiplication so that S_f and S_l are diagonal matrices. The scaled model is written as

$$\widetilde{f}(\tilde{z}) = 0 \tag{20}$$

$$\widetilde{A}s\tilde{z} = \tilde{b} \tag{21}$$

$$\tag{22}$$

where $\tilde{z} = S_v^{-1} z$, $\widetilde{f}(\tilde{z}) = S_f f(S_v \tilde{z})$, $\widetilde{A}s = S_l A_s S_v$, and $\tilde{b} = S_l b$. If the model equations are properly scaled, the condition number of

$$H = \begin{bmatrix} \widetilde{\mathbb{F}}(\tilde{z}) \\ \widetilde{A}_r \end{bmatrix} \tag{23}$$

should be reasonable low ($< 1 \times 10^6$).

It should be noted that the variable scaling has some pitfalls. A simple input-output mass balance of a two component ($j = 1, 2$) process stream is used

as an example. The resulting model has six variables and three equations and to solve the model three variable values has to be specified . The model equations are the component mass balance and sum of outlet molar fractions. The equations are written as

$$f(z) = \begin{bmatrix} \boldsymbol{x}_i F_i - \boldsymbol{x}_o F_o \\ \sum_j \boldsymbol{x}_o(j) - 1 \end{bmatrix} = 0 \tag{24}$$

The variable vector $\boldsymbol{z} = [\boldsymbol{x}_i^{\mathrm{T}}\ Fi\ \boldsymbol{x}_o^{\mathrm{T}}\ F_o]^{\mathrm{T}}$. Three specifications are added in $A_r z = b_r$. They are feed composition and feed flow ($\boldsymbol{x}_i = [0.5\ 0.5]^{\mathrm{T}}$ and $F_i = 1$) which gives

$$A_r = \begin{bmatrix} 1 & 0 & 0 & 0 & 0 & 0 \\ 0 & 1 & 0 & 0 & 0 & 0 \\ 0 & 0 & 1 & 0 & 0 & 0 \end{bmatrix} \text{ and } \boldsymbol{b}_r = \begin{bmatrix} 0.5 \\ 0.5 \\ 1 \end{bmatrix} \tag{25}$$

In this case the first order derivatives of the process model $f(\boldsymbol{z})$ and the specification matrix A_s are written as

$$H = \begin{bmatrix} \mathbb{F}(z) \\ A_s \end{bmatrix} = \begin{bmatrix} F_i & 0 & x_i(1) & F_o & 0 & x_o(1) \\ 0 & F_i & x_i(2) & 0 & F_o & x_o(2) \\ 0 & 0 & 0 & 1 & 1 & 0 \\ 1 & 0 & 0 & 0 & 0 & 0 \\ 0 & 1 & 0 & 0 & 0 & 0 \\ 0 & 0 & 1 & 0 & 0 & 0 \end{bmatrix} \tag{26}$$

The condition number of $H(\boldsymbol{z}^*) \approx 5.3$, where z^* is a solution of the process model, i.e. $f(\boldsymbol{z^*}) = 0$ and $A_s \boldsymbol{z^*} = \boldsymbol{b}_s$. If the feed composition specifications is changed to $\boldsymbol{x}_i = [0.01\ 0.99]^{\mathrm{T}}$ the condition number of $H(\boldsymbol{z}^*) \approx 6.7$. This shows that, in this case, small values of the variables $x_i(1)$ and $x_o(1)$ are not a problem. However, if variable scaling is added, such that the scaled variables have a value equal to one the condition number of $\widetilde{H} \approx 7.4 \times 10^3$. I.e. we have by improper variable scaling created a "ill conditioned" model.

On the other hand, if the molar flow Fi is increased from 1 to 100 the condition number of $H \approx 2.8 \times 10^4$. If the flow variables are scaled such that the scaled variable has a value equal to one, and the equations are scaled according to the procedure above, the condition number of the scaled model is reduced to $\widetilde{H}(z^*) \approx 8.2$. The "rule of thumb", which was applied to this model, is: be careful by assigning large variable scaling factors to variables with values close to zero. Typically, all molar fractions are by definition close to one ([0 1]) and is scaled by a factor equal to one.

The reformer model is scaled according to the procedure above and the condition number of H is reduced from 2.3×10^{12} to 3.6×10^{4}. The maximum absolute value of the elements in H is reduced from 4.8×10^{5} to 7.6 and the values of $\widetilde{H}$ corresponding to the equation-variable pairing has a value equal to one.

4 Process description

The feed to the naphtha reformer is a crude oil fraction from the refinery crude unit with a boiling range of $\approx 100-180°$C and a density of ≈ 763kg/m^3. The products are a high-octane naphtha, also called "reformate", "Gas" ($C_2 - C_4$) and hydrogen.

The overall reaction is endothermic and there is a significant temperature drop from the inlet to the outlet of the reactors. In order to compensate for this temperature drop, the reactor is separated into four sections with intermediate reheating, see figure 2. The fresh feed is mixed with hydrogen rich recycle gas and is preheated in the reactor effluent heat exchanger (E1). The feed is further heated in heater number one (H1) before it enters reactor number one (R1), and so on. The hot reactor product enters the feed preheater (E1) and is further cooled with cooling water before it enters the separator. Hydrogen rich gas is compressed, except for a small purge stream, and recycled. The liquid product from the separator (D1), a mixture of reformate and gas, is separated in a downstream distillation column.

The amount of catalyst in the four reactors is approximately in the ratio of 1:1:2:3. The reactor inlet temperatures are in the range of 770-800K.

5 Process modeling

The increase in octane number is due to a conversion of paraffins and naphthenes in the feed into aromatics.

The components in the process are lumped into five pseudo components. These are hydrogen (H), "Gas" $C_2 - C_4$ (G), paraffines (P), naphthenes (N) and aromatics (A). The thermodynamic properties of these pseudo components are described in appendix A.

The justification for this simplification is that the carbon number of the molecules does not change in the two reactions (27) and (28). For example, a C_7 naphthene is converted to a C_7 aromatic and a C_7 paraffin is converted

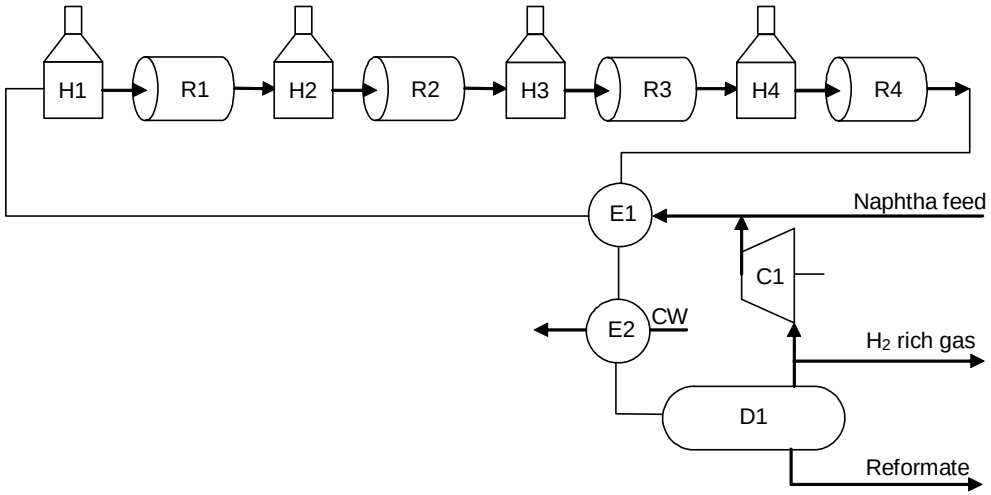

Figure 2: Naphtha reformer

to a C_7 naphthene.

This conversion is described by four main reactions (Smith, 1959):

1. Dehydrogenation of naphthenes to aromatics
2. Dehydrocyclization of paraffins to naphthenes
3. Hydrocracking of naphthenes to light ends
4. Hydrocracking of paraffins to light ends

The simplified naphtha reforming kinetics, as described in Smith (1959), are written as

$$\mathrm{N} \overset{r_1}{\rightleftharpoons} \mathrm{A} + 3\mathrm{H_2} \tag{27}$$

$$\mathrm{N} + \mathrm{H_2} \overset{r_2}{\rightleftharpoons} \mathrm{P} \tag{28}$$

$$\mathrm{N} + 2\mathrm{H_2} \overset{r_3}{\rightarrow} 2\mathrm{G} \tag{29}$$

$$\mathrm{P} + \mathrm{H_2} \overset{r_4}{\rightarrow} 2\mathrm{G} \tag{30}$$

with the stoichiometric matrix $\boldsymbol{N}$

$$\boldsymbol{N} = \begin{bmatrix} 3 & 0 & 0 & -1 & 1 \\ -1 & 0 & 1 & -1 & 0 \\ -2 & 2 & 0 & -1 & 0 \\ -1 & 2 & -1 & 0 & 0 \end{bmatrix} \tag{31}$$

where the columns refer to the components H, G, P, N and A. The reaction rates are,

$$
\begin{aligned}
r_1 &= k_{f_1} p_N - k_{r_1} p_A p_{H_2}^3 && (32)\\
r_2 &= k_{f_2} p_N p_{H_2} - k_{r_2} p_P && (33)\\
r_3 &= k_{f_3} p_N / p && (34)\\
r_4 &= k_{f_4} p_P / p && (35)
\end{aligned}
$$

where p_x is the partial pressure of component x and p is the overall reactor pressure.

For the forward and reverse rate constants, k_f and k_r, an Arrhenius type of rate expression is assumed

$$
k_f = k_{0f} e^{\left(\frac{-E_f}{RT}\right)} \qquad k_r = k_{0r} e^{\left(\frac{-E_r}{RT}\right)} \tag{36}
$$

where the activation energy E is dependent on the catalyst and k_{0f} is dependent of the molarity of the reaction (Bommannan et al., 1989). R is the universal gas constant. Reaction 1 is endothermic and reaction 2-4 are exothermic. Reaction 1 dominates such that the overall reaction is endothermic.

The model equations are organized in unit models. Appendix B gives a detailed description of all unit models used in this paper. A description of the modeling framework, with case studies, can be found in Lid and Skogestad (2006).

The details of the reformer model are shown in figure 3. The liquid feed S_1 is mixed with recycle gas S_{55}. The resulting vapor $S_(2)$ and a liquid $S_(3)$ outlet stream enters the reactor effluent heat exchanger E1. The E1 outlet streams S_4 then enters the first heater and reactor section. The heaters are modeled as a direct heat input and each of the four reactors is modeled using ten CSTRs in series with even distribution of catalyst. Heat exchanger E2 and separator D1 is modeled using the same flash unit model . The reason is that the flash calculation is needed in the heat exchanger to compute the enthalpy of the outlet streams.

In addition variables and equations for Reformate octane number (RON), feed hydrogen to hydrocarbon ratio, and some mass flows are added as internal variables in a "dummy" unit model. The mass flows are the feed mass flow, Reformate, gas and hydrogen product mass flow and the recycle gas mass flow

The mass balance of a reactor element is written as

$$
F_i \boldsymbol{x}_i - F_o \boldsymbol{x}_o + \boldsymbol{N} A_c^{\mathrm{T}} \boldsymbol{r}(T_o, P_o) m_c = 0 \tag{37}
$$

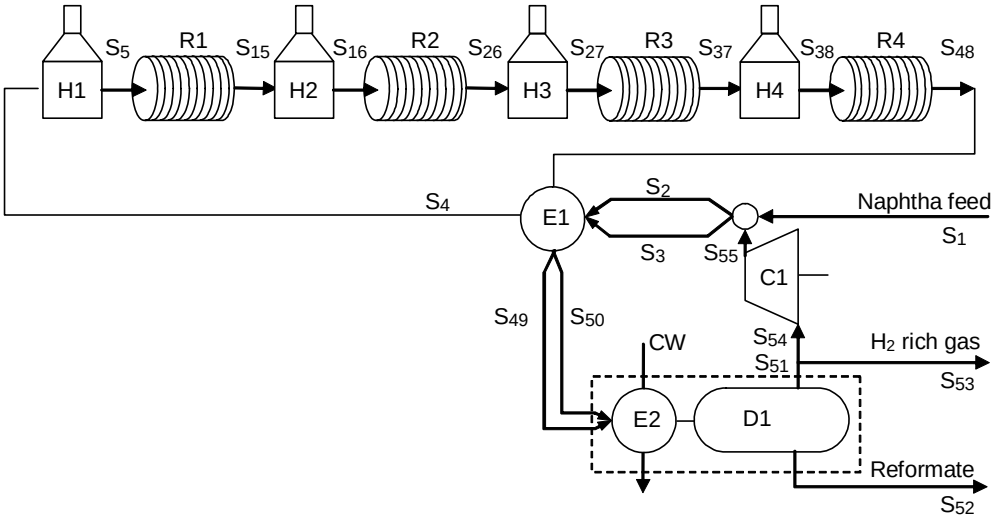

Figure 3: Model details of the naphtha reformer

where F_i,$\boldsymbol{x}_i$ and F_o,$\boldsymbol{x}_o$ is the inlet and outlet stream molar flow and molar component fractions, m_c is the mass of catalyst, an A_c is the catalyst activity parameter, which is expected to be close to one.

The resulting model and specifications are written

$$\begin{aligned} f(z) &= 0 \\ A_s z &= b_s \end{aligned} \tag{38}$$

There are $n_z = 501$ variables z and $n_f = 442$ equations in the reformer process model $f(z) = 0$. These are listed in table 1 and the equations 2.

The remaining $n_z - n_f = 59$ variables need to be specified and are added as $n_s = 59$ rows in A_s with the corresponding specification value in b_s.

The catalyst efficiency factors for all CSTRs within one reactor where constrained to have equal values. This is incorporated as 36 linear constraints in A_s.

$$A_{c_i} - A_{c_{i+1}} = 0 \text{ for } i = 1...9, 10...19, 20...29, 30...39 \tag{39}$$

Values for feed condition, reactor temperatures, recycle rate, heat transfer coefficients and compressor efficiency is also specified by addition of rows in A_s and corresponding values in b_s. The specified variables with corresponding values for the 23 remaining degrees of freedom is shown in table 3.

The selection of specification variables is not unique and other valid variable combinations exists. In order to have a unique solution the matrix of first order derivatives of the nonlinear constraints and the linear constraint matrix must have full rank.

In order to reduce the computational load in solving the model the first order derivatives are calculated analytically.

$$\mathbb{F}(z) = \frac{\partial f(z)}{\partial z} \tag{40}$$

5.1 Nominal case

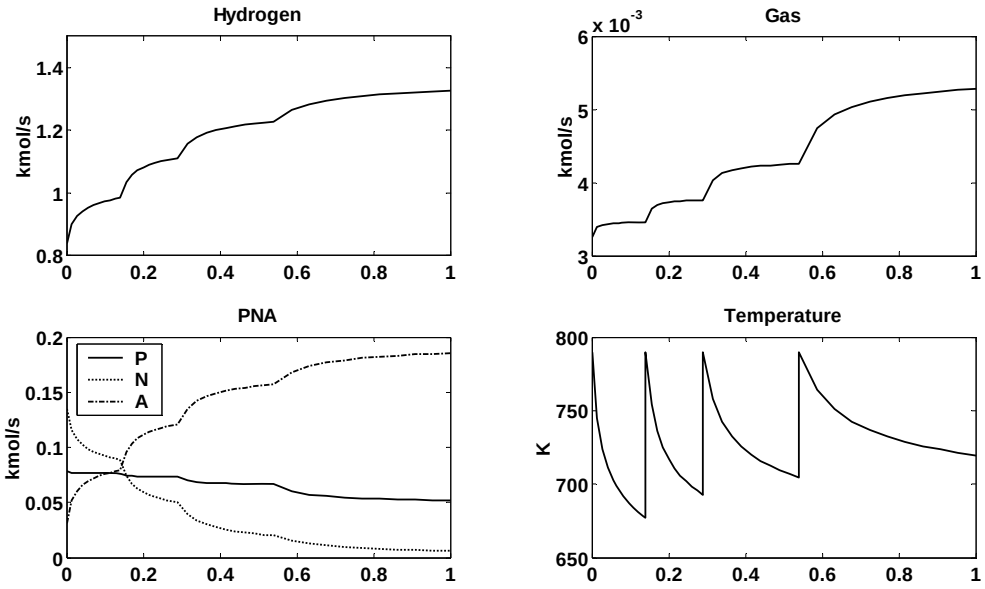

Figure 4: Nominal flows and temperature in reactors

Figure 4 shows the molar flows of each component trough the four reactors as a function of normalized catalyst mass. The figure shows a net production of hydrogen and gas. The largest amount of hydrogen is produced in reactor one and the largest amount of gas is produced in reactor four. The dominating reaction in reactor number one is conversion of naphthenes to aromatics is and the dominating reaction in reactor number four is conversion of paraffines to naphthenes. The large temperature drop in reactor one is due to the large heat of reaction for the conversion of naphthenes to aromatics.

Process streams			
x		Molar fraction	NC
F	kmol/s	Molar flow	1
T	K	Temperature	1
P	bar	Pressure	1
		Total: $(NC+3)\times 55$	440
Heaters			
Q	kW	Duty	1
		Total: 1×4	4
Reactors			
A_c		Catalyst efficiency factor (one for each CSTR)	10
		Total: 4×10	40
Heat exchanger E1			
Q	kW	Duty	1
U_1	kW/m^2/K	Heat transfer coefficient	1
Heat exchanger E2 and condenser			
Q	kW	Duty	1
U_2	kW/m^2/K	Heat transfer coefficient	1
F_{CW}	kmol/s	Cooling water molar flow	1
T_{CW_i}	K	Cooling water inlet temperature	1
T_{CW_o}	K	Cooling water outlet temperature	1
Compressor			
W	kW	Work	1
ψ		Efficiency	1
T_s	K	Reversible compression outlet temperature	1
Additional constraints			
RON		Reformate octane number	1
H_2/HC		Hydrogen to hydrocarbon ratio	1
$\widetilde{F}_1$	t/h	Feed mass flow	1
$\widetilde{F}_{55}$	t/h	Recycle mass flow	1
$\widetilde{F}_{53}$	t/h	Vapor product mass flow	1
$\widetilde{F}_{52}$	t/h	Reformat product mass flow	1
$\widetilde{F}_{53}(H_2)$	t/h	Hydrogen product mass flow	1
		Total:	$n_z = 501$

Table 1: Reformer model variables

Unit model	n_{fi}	Total
Heater	$NC+3$	$(NC+3)\times 4$
CSTR	$NC+3$	$(NC+3)\times 40$
Heat exchanger E1	$3NC+10$	$3NC+10$
Heat exchanger E2 and condenser	$2NC+8$	$2NC+8$
Compressor	$NC+4$	$NC+4$
Vapor/liquid feed mixer	$2NC+6$	$2NC+6$
Stream split	$2NC+5$	$2NC+5$
Additional constraints	7	7
Total	$54NC+172=$	$n_f=442$

Table 2: Reformer model equations

Description	Variable	Value
Catalyst efficiency factor reactor 1	A_{c1}	1
Catalyst efficiency factor reactor 2	A_{c11}	1
Catalyst efficiency factor reactor 3	A_{c21}	1
Catalyst efficiency factor reactor 4	A_{c31}	1
E1 heat transfer coefficient	U_1	560
E2 heat transfer coefficient	U_2	200
E2 cooling water flow	F_{CW}	5
E2 cooling water inlet temperature	T_{CW_i}	288
Compressor efficiency	ψ	0.75
Feed component molar fraction	$x_1(H)$	0
Feed component molar fraction	$x_1(G)$	0
Feed component molar fraction	$x_1(P)$	0.32
Feed component molar fraction	$x_1(N)$	0.56
Feed component molar fraction	$x_1(A)$	0.12
Feed mass flow	$\widetilde{F}_1$	85
Feed temperature	T_1	358
Reactor 1 inlet temperature	T_5	790
Reactor 2 inlet temperature	T_{16}	790
Reactor 3 inlet temperature	T_{27}	790
Reactor 4 inlet temperature	T_{38}	790
Compressor recycle mass flow	$\widetilde{F}_{55}$	8.0
Vapor product pressure	P_{53}	7.9
Liquid product pressure	P_{52}	8.0

Table 3: Simulation variable specifications

Other key variables like heater duties and product yields are listed in table 4. The reformate and vapor yields are 94.57% and 5.43% respectively. If the

Variable		Value	Unit
Heater 1 duty	Q_{H_1}	8818	kW
Heater 2 duty	Q_{H_2}	11865	kW
Heater 3 duty	Q_{H_3}	10350	kW
Heater 4 duty	Q_{H_4}	9196	kW
Compressor duty	W_C	682	kW
Heat exchanger E1 duty	Q_{E_1}	37596	kW
Heat exchanger E2 duty	Q_{E_2}	6865	kW
Feed H_2/HC ratio	H_2/HC	3.48	
Reformate octane number	RON	102.4	
Reformate product flow	$\widetilde{F}_{52}$	80.4	t/h
Vapor product flow	$\widetilde{F}_{53}$	4.6	t/h

Table 4: Simulation results

vapor stream is split into hydrogen and gas the hydrogen and gas yield are 4.13% and 1.30% respectively.

6 Data reconciliation results

The naphtha reformer process has in total $n_y = 26$ measured values. These are feed, product and recycle gas analyzers, feed product and recycle gas mass flow measurements and various temperature measurements. All the measurements are listed in table 6

The limitation of equal catalyst efficiency factor within each reactor added as rows in A_r. The feed hydrogen and gas content is known to be practically equal to zero and specifications for $x_1(1) = 0$ and $x_1(2) = 0$ is added in A_r. The remaining degrees of freedom then equals 21.

For the reformer model we have that

$$\text{rank} \begin{bmatrix} H_r(z^*) \\ U \end{bmatrix} = 498 \tag{41}$$

using equation 6. This indicates three unobservable variables.

The condenser liquid outlet pressure is not specified and the liquid stream is not connected to any downstream unit. This variable is not present in any of the model equations and is clearly unobservable.

There are no measurements of the cooling water inlet or outlet flow or temperature.

In order to make all variables observable the values of P_{52}, F_{CW} and T_{CW_i} are specified by adding three linear constraints in A_r and the corresponding values in b_r. The matrix in equation 41, with the addition ow three new rows in A_r, has rank equal to n_z and all variables are now, by definition in the equation , observable. The degrees of freedom is now reduced from 21 to 18.

It is verified, using equation 7, that all measurements in the the reformer process are redundant.

The standard deviation if the estimated values $\sigma_{y_i} = \sqrt{\Sigma_y(i,i)}$ is shown in table 6.

There are almost no reduction of uncertainty in the estimate of the reactor inlet or outlet temperatures, compared with the uncertainty of the measured values. The feed and product mass flows uncertainty is reduced by approximately 30%. The compressor inlet temperature, separator outlet temperature and recycle gas hydrogen content has a large reduction of uncertainty. This is probably due to a oversimplification in the modeling of the separator and recycle gas system (i.e. model error).

The values and uncertainties of the heat exchangers heat transfer coefficient, reactor and compressor efficiency are shown in table 5.

Description	Variable	Value	σ
Catalyst efficiency factor reactor one	A_{c1}	1.30	0.16
Catalyst efficiency factor reactor one	A_{c2}	0.59	0.17
Catalyst efficiency factor reactor one	A_{c3}	1.36	0.21
Catalyst efficiency factor reactor one	A_{c4}	0.93	0.20
E1 heat transfer coefficient	U_1	515	165
E2 heat transfer coefficient	U_2	200	1362100
Compressor efficiency	ψ	0.76	0.10

Table 5: Uncertainties of unmeasured variables

On average the uncertainty in these variables are 10-35% of the actual value except for the estimate of U_2. The uncertainty of U_2 shows that this variable is not practically observable.

The reconciliation problem was solved for 21 different data sets, sampled during a period of two years of operation. The reconciled solution shown in table 6 is from data set number 12. Gross errors are detected for the measured values marked with *. The outlet temperatures of reactor four and of heat exchanger E1 have a gross error detected in all 21 data sets. The

Measurement	Var.	Meas. y	Rec. Uz_r	Std. σ_m	Std. σ_y	Unit
Feed P molar fraction	$x_1(3)$	0.32	0.32	0.01	0.010	
Feed N molar fraction	$x_1(4)$	0.56	0.56	0.01	0.010	
Feed A molar fraction	$x_1(5)$	0.12	0.12	0.01	0.010	
Feed temperature	T_1	358.5	360.8	3.0	2.72	K
E1 cold side inlet temperature	T_2	344.5	338.2	3.0	1.49	K
E1 cold side outlet temperature	T_4	706.6	706.6	3.0	2.71	K
Heater 1 outlet temperature	T_5	794.0	794.3	3.0	2.96	K
Reactor 1 outlet temperature	T_{15}	*649.1	670.0	3.0	2.97	K
Heater 2 outlet temperature	T_{16}	788.6	788.9	3.0	2.96	K
Reactor 2 outlet temperature	T_{26}	704.0	703.8	3.0	2.96	K
Heater 3 outlet temperature	T_{27}	798.4	798.8	3.0	2.96	K
Reactor 3 outlet temperature	T_{37}	698.6	698.4	3.0	2.96	K
Heater 4 outlet temperature	T_{38}	797.8	798.2	3.0	2.96	K
Reactor 4 outlet temperature	T_{48}	*763.6	722.8	3.0	2.71	K
E1 hot side outlet temperature	T_{50}	*385.4	353.5	3.0	1.98	K
Separator D1 pressure	P_{51}	7.93	7.89	0.2	0.16	bar
Separator D1 outlet temperature	T_{52}	292.2	294.1	3.0	0.51	K
Recirculation gas H molar frac.	$x_{54}(1)$	0.90	0.99	0.1	0.0002	
Compressor inlet temperature	T_{54}	294.2	294.1	3.0	0.51	K
Compressor outlet temperature	T_{55}	323.0	324.4	3.0	2.92	K
Compressor outlet pressure	P_{55}	10.3	10.3	0.2	0.14	bar
Reformate product octane number	RON	103.9	103.7	1.0	0.72	
Feed mass flow	$\widetilde{F}_1$	88.0	87.1	3.0	2.13	t/h
Compressor outlet mass flow	$\widetilde{F}_{55}$	10.1	9.78	1.0	0.67	t/h
Vapor product mass flow	$\widetilde{F}_{53}$	6.54	4.96	1.0	0.17	t/h
Reformate product mass flow	$\widetilde{F}_{52}$	80.3	82.1	3.0	2.02	t/h

Table 6: Measured variables, measured values, reconciled values and measurement uncertainty for data set no. 12

outlet temperatures of reactors one and two have gross errors detected in 13 and 14 of the data sets, respectively. The compressor mass flow has a gross error detected in three data sets and the feed temperature has a gross error detected in one data set.

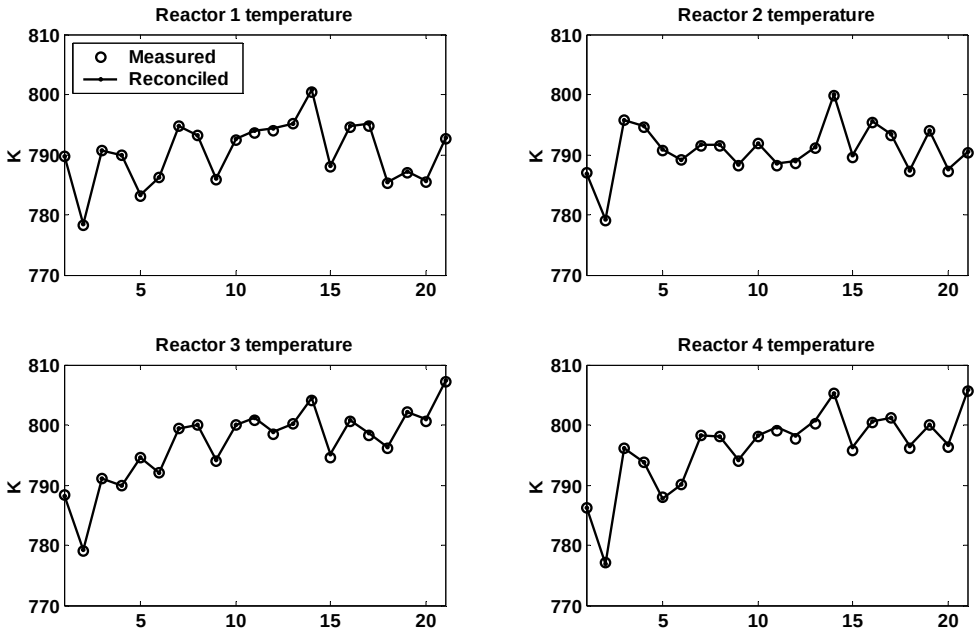

Figure 5: Reconciled reactor inlet temperatures for the 21 data sets

Figure 5 shows the measured and reconciled reactor inlet temperatures. The adjustments of the catalyst efficiency factors contributes to a almost perfect fit to the measured data. We have the highest reaction rate, and influence on the other measured values, at the inlet of the reactor and this may be the reason why the error in temperature drop over each reactor is assigned to the reactor outlet temperatures.

There are large measurement errors in the reactor outlet temperatures, as shown in figure 6. The outlet temperature of reactor one and two have gross errors in most data sets but also some data points almost zero measurement error. The outlet temperature of reactor number four has a almost fixed bias in all data sets. As a curiosity, the outlet temperature of reactor three, which has a almost zero measurement error in all data points is at the refinery "accepted" as an untrustworthy measurement.

The estimated catalyst efficiencies for all data sets are shown in figure 7.

Ideally, the the catalyst efficiency factors A_c should be close to one in all

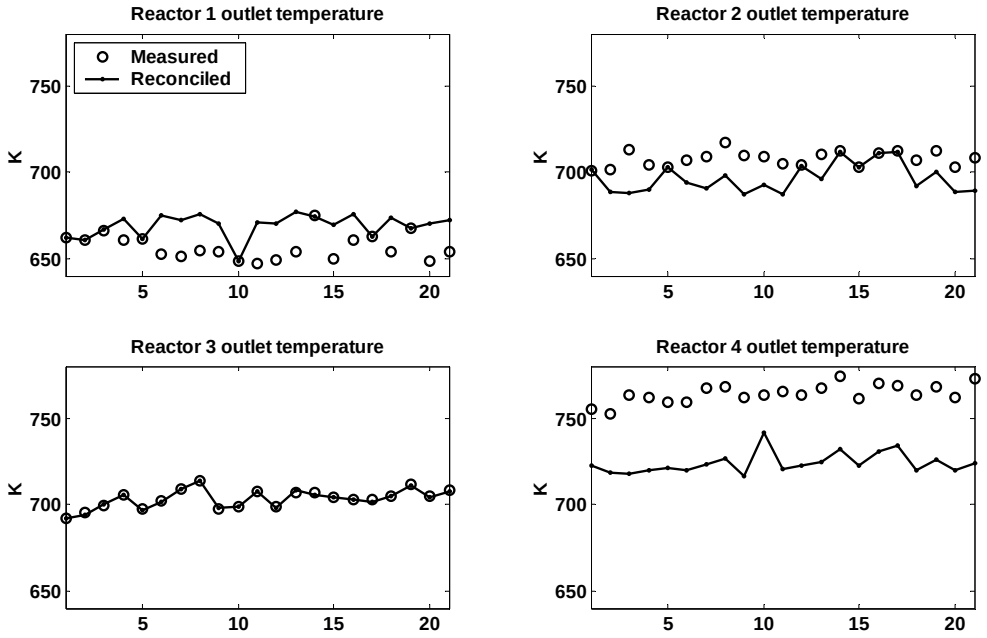

Figure 6: Reconciled reactor outlet temperatures for the 21 data sets

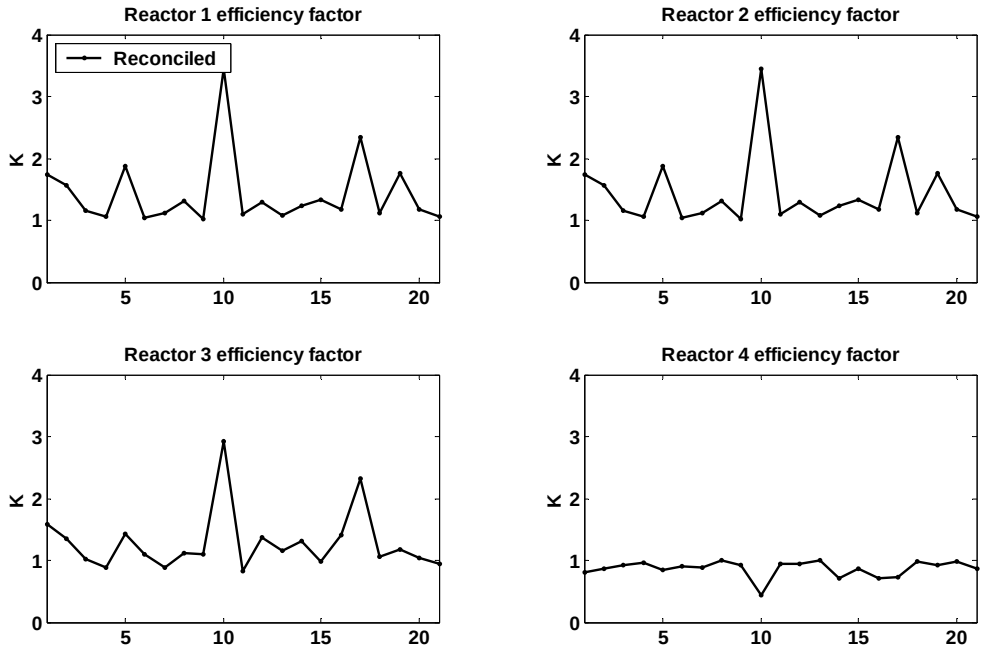

Figure 7: Reactor efficiencies A_c for the 21 data sets

data sets but due to variation in the catalyst circulation some changes in A_c are expected. In periods, where the catalyst regenerator is shout down, the unit may run for several days with no catalyst circulation . In these periods the catalyst efficiency will decrease due to a coke build up on the catalyst.

The values of A_c have large variations in data points 5, 10, 17 and 19. There is no clear reason for this and the data at these points does not differ significantly from the others. A observation is that the measurement error of reactor one outlet temperature is almost zero at these points but this is also true for data point 1, 2, 3 and 14.

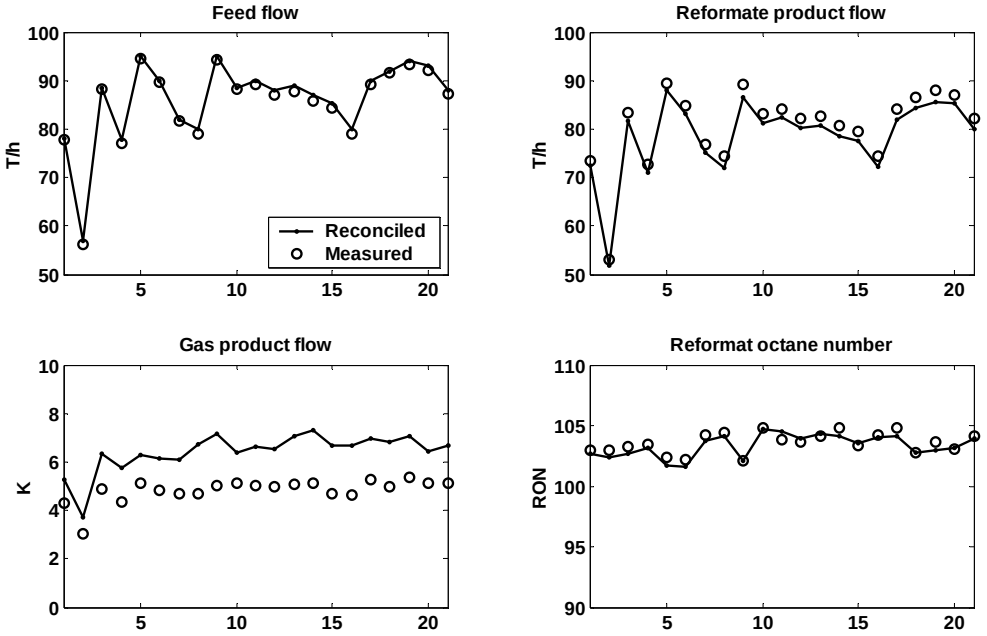

Figure 8: Reconciled mass flows and product quality

The average deviation of measured and reconciled feed, reformate and gas mass flows, as shown in figure 8, are 0.7t/h, -1.93t/h and 1.59t/h respectively. The octane reconciled and measured value deviation is -0.25. The reconciled gas mass flow is persistently lower than the measured value and even if no gross errors where detected in the measured value the presence of a systematic error is clear.

7 Optimal operation

Optimal operation is defined as the operation which maximizes the profit, given the current process condition and operating constraints. The current process condition is estimated using data reconciliation, $\boldsymbol{z}_r$ and the optimal operation is calculated by minimization of a cost or negated profit function subject to the process model, fixed variables and operating constrains. The optimization problem is written as

$$\begin{aligned} \min_{z} \quad & J(z) \\ \text{s.t.} \quad & f(z) = 0 \\ & A_{opt} z = b_{opt} \\ & z_{opt\,\min} \leq z \leq z_{opt\,\max} \end{aligned} \tag{42}$$

where $J(z) = -p(z)^{\mathrm{T}} z$. In most cases p is a vector of fixed prices of feed, products and energy.

Values for variables describing feed conditions like composition and temperature, heat exchanger heat transfer coefficients and compressor efficiency are fixed and set equal to their reconciled values. These values are specified using the linear equality constraints $A_{opt} z = b_{opt}$ in (42).

Operating constraints like maximum feed flow, maximum pressure, maximum temperature and minimum product octane are added as upper and lower bounds on the variables in $z_{opt\,\min}$ and $z_{opt\,\max}$.

The number of degrees of freedom $n_z - n_f - n_{opt} = 7$ where the number of variables $n_z = 501$, $n_f = 442$ and the number of rows in A_{opt}, $n_{opt} = 52$. The specified or fixed values added in A_{opt} are 40 catalyst efficiency factors, 2 heat exchanger heat transfer coefficients, compressor efficiency, feed temperature and feed composition (NC=5), reformate outlet pressure, cooling water flow and cooling water inlet temperature.

7.1 Cost function

The feed, product and energy price in problem 42 are shown in table 7. The elements of p, corresponding with the variables in table 7, are updated with their respective price. All other elements of p equals zero. The most important operational constraints are shown in table 7 as maximum and minimum variable values.

Description	Value	Unit	Variable
Feed cost	-60	\$/t	$\widetilde{F}_1$
Reformate cost	100	\$/t	$\widetilde{F}_{52}$
Gas cost	50	\$/t	$\widetilde{F}_{53}$
Energy cost	-0.0015	\$/kW	$Q_{H1}, Q_{H2}, Q_{H3}, Q_{H4}, W$

Table 7: Economic data

7.2 Active constraints

Two operational cases, which both are common operational regimes for a naphtha reformer unit in a refinery, are analyzed.

In case 1, the product price is high and reformer throughput is maximized.

In case 2, the product price is high and reformer throughput is minimized.

The naphtha reformer is the main producer of hydrogen at the refinery and may not be shout down even if the product price is low and the unit profit is negative. In order to secure the availability of hydrogen a low bound is added on the reformer unit hydrogen production.

Description	Variable	Unit	Min.	Max.	Rec.	Case 1	Case 2	Price
Feed flow	$\widetilde{F}_1$	t/h			89.2	95.6	84.1	-60.0
Reformate flow	$\widetilde{F}_{52}$	t/h			84.2	90.6	79.7	**100.0
Gas flow (LPG)	$\widetilde{F}_{53}(G)$	t/h			1.2	1.0	0.9	50.0
H_2 mass flow	$\widetilde{F}_{53}(H)$	t/h	3.5		3.8	4.0	*3.5	
Reformat octane	RON		103.0		103.9	*103.0	*103.0	
Reactor 1 temp.	T_5	K		810.0	794.0	790.7	794.1	
Reactor 2 temp.	T_{16}	K		810.0	788.6	782.7	788.8	
Reactor 3 temp.	T_{27}	K		810.0	801.2	799.9	798.8	
Reactor 4 temp.	T_{38}	K		810.0	799.6	791.6	780.4	
Heater 1 duty	Q_1	MW		9.5	9.3	*9.5	8.6	-0.015
Heater 2 duty	Q_2	MW		13.0	12.7	*13.0	12.2	-0.015
Heater 3 duty	Q_3	MW		13.0	12.1	*13.0	11.3	-0.015
Heater 4 duty	Q_4	MW		10.0	10.0	*10.0	7.6	-0.015
Compressor duty	W	MW			0.88	0.48	0.39	-0.015
Feed H_2/HC ratio	H2/HC		3.0	5.0	*3.0	*3.0		
Separator pres.	P_{53}	bar	8.0	10.0	8.0	*10.0	*10.0	
Profit		\$/h			2638	2883	-249	

Table 8: Optimal operation corresponding to data set 11 (* = active constraint, **= in case 2 the price of reformate is 65\$/t)

The most important variables of the optimal operation for case 1 and 2 is

shown in table 8.

In case 1, the operation is constrained on reformate RON, heater duty, feed hydrogen to hydrocarbon ratio and pressure. The improvement in profit, compared to the reconciled solution, is in this case 244\$/h (2.1×10^6 \$/year). Of this 259\$/h is gained as a result of increased feed flow and a reformate yield improvement of 0.43%. 14.1 \$/h is gained by reduction of energy consumption. The yield improvement is mainly due to reduced temperatures in the reactors and reduced reformate RON.

In case 2, the operation is constrained on reformate RON, hydrogen product mass flow, feed hydrogen to hydrocarbon ratio and pressure.

The marginal values of the active constraints are computed by adding a small change to the constraint value and observe the corresponding change in the profit function at the new optimal conditions.

Description	Variable	Case 1	Case 2
Reformat octane	RON	-124	-13
Feed H_2/HC ratio	H2/HC	-24	-5.0
Separator pres.	P_{53}	-0.44	-1.9
H_2 mass flow	$\widetilde{F}_{53}(H)$	-	-79
Heater 1 duty	Q_1	-60	-
Heater 2 duty	Q_2	-60	-
Heater 3 duty	Q_3	-60	-
Heater 4 duty	Q_4	-60	-

Table 9: Active constraints marginal values corresponding to data set 11 (\$/unit)

In order to operate the process the seven degrees of freedom has to be specified or fixed. These specifications are implemented as controlled variables. The degrees of freedom are related to the heat input to the four heaters and the mass flow of feed, recycle and H_2 rich gas. The basic control layer includes heater duty control, feed flow control and pressure control.

In case 1, the seven active constraints are selected as controlled variables.

In case 2, the four active constraints are selected as controlled variables. These are reformate RON, hydrogen product mass flow, feed hydrogen to hydrocarbon ratio and pressure. The remaining three control variables has to be selected such that the economic loss is small. The temperature difference of the inlet of the four reactors are three such control variables. If three control loops are implemented such that all reactor have equal inlet temperatures the economic loss, compared to having optimal inlet temperatures, is

small (0.005$/h). This is also consistent with the equal marginal values of the heater duties in case 1 shown in table 9. I.e. "self optimizing control" is achieved by adding the reactor difference temperatures as control variables with a zero set point.

The constraint marginal values also shows that in case 1 the reformate RON is the most important variable to keep close to its minimum value. Similar, the hydrogen mass flow is the most important variable in case 2.

Manipulated variables	Controlled variables Case 1	Controlled variables Case 2
Feed flow	Reformate RON	H_2 product flow
Heater 1 duty	Fixed set point	Reformate RON
Heater 2 duty	Fixed set point	T_{R1_i}-T_{R2_i}
Heater 3 duty	Fixed set point	T_{R1_i}-T_{R2_i}
Heater 4 duty	Fixed set point	T_{R1_i}-T_{R2_i}
Pressure	Fixed set point	Fixed set point
Compressor work	H_2/HC ratio	H_2/HC ratio

Table 10: Control structure (controlled and manipulated variable pairing)

Table 10 shows the control structure which yields close to optimal operation for the two operational cases.

8 Discussion

The measured recycle gas hydrogen mole fraction is 0.90 and the reconciled value is 0.99. This error is mainly due to model error and the simplification of the hydrocarbon light end components. In the model, G does not evaporate at the process conditions in the separator. In the real process a molar fraction of 0.04 C_1 and C_2 hydrocarbons are present in the recycle gas. Also a molar fraction of 0.03 C_3+ is present. This indicates a non ideal behavior in the separator with some entrainment of heavier hydrocarbons. The pseudo component G may give a sufficiently accurate description of the reactions nut seams to be to simple to give a good description of the separator and recycle system. The uncertainty of the recycle gas analyzer is set at a high value (0.1) since the "measurement error" in this case is mainly due to modeling error.

The uncertainty of the heat transfer coefficient of the heat exchanger two $U2$ is large and practically not observable even if observability test in equation

6 shows that it is observable. A singular value decomposition of the matrix may give more practical information of the variable observability.

$$USV^{\mathrm{T}} = \begin{bmatrix} \widetilde{H}_r(z^*) \\ \widetilde{U} \end{bmatrix} \tag{43}$$

The singular values s_i, along the diagonal of S, have values $1.02 \times 10^{-3} < s_i < 23.2$ except for one value which equals 6.0×10^{-7}. The corresponding right hand side singular vector has all elements close to zero except for the element corresponding to the variable U_2, which is close to one $(1 - s(U_2) < 4 \times 10^{-9})$. If $r = USV^{\mathrm{T}}\tilde{z}$ a change in the variable U_2 has a small effect on the residual r, compared to the other variables. Changes in U_2 will also have a small effect on the the data reconciliation objective. This may be the reason that the reconciled value of U_2 is not changed and always close to its initial value in all of 21 data sets.

9 Conclusions

A refinery naphtha reformer is successfully modeled using a simple unit model structure. Necessary scaling of variables an equations improves the numerical properties of the model. The condition number of the model equations are reduced from 2.3×10^{12} to 3.6×10^4. The model equations are solved using seven iterations using "best guess" initial values.

The model is fitted to 21 different data points using data reconciliation. The results show significant variation in catalyst efficiency parameters and deviation in reactor outlet temperatures. A good fit in one data set is not sufficient to claim that the model is a good description of the process.

The data reconciliation problem is analyzed and unobservable variables are identified. This example also shows that if a variable is defined as observable, by the observability test, it still may be practically unobservable. This is consistent with the computed uncertainly of the estimate, where the "barely observable variable" has a uncertainty 6800 times its value.

The computed uncertainty of the measured values shows that the uncertainty in the estimate of reactor inlet and outlet temperatures, compared with the measurement, is typically reduced by 2%. The uncertainty in mass flows is typically reduced by 30%.

Optimal operation is computed for two common operational cases defined by a low or high product price. The optimum operation has in case 1 seven

active constraints and in case 2 four active constraints. In both cases active constraints are selected as controlled variables. In case 2, three degrees of freedom are unconstrained. The remaining three degrees of freedom are specified by adding three reactor inlet temperature differences as "self optimizing control variables".

A Thermodynamics

A set of simplified properties calculations for the five pseudo components, Hydrogen (H), Gas (G), Paraffines (P), Naphthenes (N) and Aromatics (A), are used in the reformer process model. The number components in the model NC equals the number of of pseudo components, i.e. $NC = 5$.

The properties of H is set equal to the properties of hydrogen (H_2). The properties of G is equal to the properties of a mixture with equal amount of Ethane, Propane and Butane ($C_2H_6, C_3H_8, C_4H_{10}$). P has the same properties as Heptane (C_7H_{16}), N the same properties as Cycloheptane (C_7H_{14}) and A the same properties as Toluene (C_7H_8).

The naphtha reformer feed has a average PNA composition of 35%, 52% and 13% respectively. The average liquid density is 763kg/m^3 and the average 50% boiling point is 387K.

The properties of a mixture of the above defined pseudo components, with the same PNA ratio has density equal to 777kg/m^3 and boiling point equal to 384.5K. This shows that the selected properties for the pseudo components gives a reasonable fit to the properties of the real process stream.

A.1 Enthalpy

The specific enthalpy of liquid and vapor is calculated using the specific heat capacity. The specific enthalpy of liquid is calculated as

$$h_l(\boldsymbol{x}, T) = \boldsymbol{x}^{\mathrm{T}} \boldsymbol{C}_{p_l}(T - T_r) \tag{44}$$

where $\boldsymbol{x}$ is the molar fractions of each component in the mixture and $\boldsymbol{C}_{p_l}$ is a $NC \times 1$ vector holding the value of specific heats of each component. For the liquid phase the specific heat is a constant value. T and T_r is the actual and reference temperature respectively. The reference temperature $T_r = 273.15$K

The specific enthalpy of a vapor is calculated as

$$h_v(\boldsymbol{x}, T) = \boldsymbol{x}^{\mathrm{T}} \boldsymbol{h}_{vl} + \boldsymbol{x}^{\mathrm{T}} \int_{T_r}^{T} \boldsymbol{C}_{p_v}(T) dT \tag{45}$$

where the heat of vaporization $\boldsymbol{h}_{vl}$ is a $NC \times 1$ containing the heat of vaporization, at the reference temperature, of each component. The specific heat of each component is described by a fifth order polynomial function.

$$C_{p_v} = a_0 + a_1 T^1 + a_2 T^2 + a_3 T^3 + a_4 T^4 + a_5 T^5 \tag{46}$$

where the coefficients $a_0 ... a_5$ are estimated from properties data tables obtained from NIST (2005).

The specific enthalpy of vapor is calculated as

$$\begin{aligned} h_v(\boldsymbol{x}, T) = \boldsymbol{x}^{\mathrm{T}} \boldsymbol{h}_{vl} + \boldsymbol{x}^{\mathrm{T}} \hat{\boldsymbol{a}}_0 (T - T_r) + \frac{1}{2} \boldsymbol{x}^{\mathrm{T}} \hat{\boldsymbol{a}}_1 (T - T_r)^2 \\ + \frac{1}{3} \boldsymbol{x}^{\mathrm{T}} \hat{\boldsymbol{a}}_2 (T - T_r)^3 + \frac{1}{4} \boldsymbol{x}^{\mathrm{T}} \hat{\boldsymbol{a}}_3 (T - T_r)^4 \\ + \frac{1}{5} \boldsymbol{x}^{\mathrm{T}} \hat{\boldsymbol{a}}_4 (T - T_r)^5 + \frac{1}{6} \boldsymbol{x}^{\mathrm{T}} \hat{\boldsymbol{a}}_5 (T - T_r)^6 \end{aligned} \tag{47}$$

where $\hat{\boldsymbol{a}}_0 ... \hat{\boldsymbol{a}}_6$ are $NC \times 1$ vectors of polynomial coefficients.

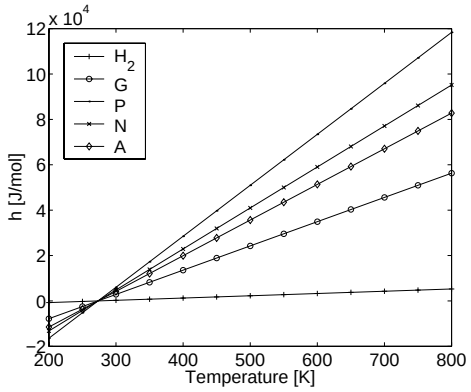

Figure 9: Liquid enthalpy plot

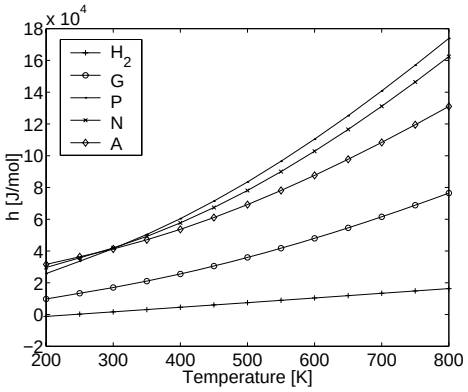

Figure 10: Vapor enthalpy plot

Figure 9 and 10 shows the enthalpy of the five pseudo components in the temperature range of 200-800K.

A.2 Entropy

The entropy is a function of composition, temperature an pressure. It is used in the compressor unit model and is calculated for the vapor phase only. The entropy of a gas with ideal gas behavior is written as

$$s_v(\boldsymbol{x}, T, P) = \boldsymbol{x}^{\mathrm{T}} \int_{T_r}^{T} \frac{\boldsymbol{C}_{p_v}(T)}{T} dT - R \log(P/P_r) \tag{48}$$

and the entropy function is calculated as

$$\begin{aligned} s_v(\boldsymbol{x}, T, P) = \boldsymbol{x}^{\mathrm{T}}\hat{\boldsymbol{a}}_0 \log(\frac{T}{T_r}) + \boldsymbol{x}^{\mathrm{T}}\hat{\boldsymbol{a}}_1(T - T_r) \\ + \frac{1}{2}\boldsymbol{x}^{\mathrm{T}}\hat{\boldsymbol{a}}_2(T - T_r)^2 + \frac{1}{3}\boldsymbol{x}^{\mathrm{T}}\hat{\boldsymbol{a}}_3(T - T_r)^3 \\ + \frac{1}{4}\boldsymbol{x}^{\mathrm{T}}\hat{\boldsymbol{a}}_4(T - T_r)^4 + \frac{1}{5}\boldsymbol{x}^{\mathrm{T}}\hat{\boldsymbol{a}}_5(T - T_r)^5 \\ - R\log(P/P_r) \end{aligned} \tag{49}$$

Figure 11 shows the entropy of the five pseudo components, at fixed pressure,

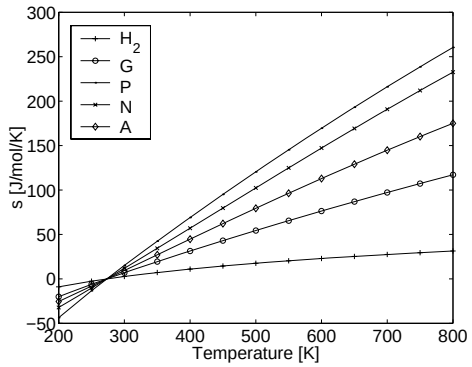

Figure 11: Vapor entropy plot at constant pressure, $P = P_r$.

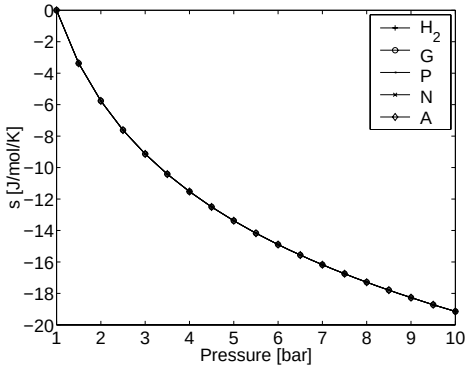

Figure 12: Vapor entropy plot at constant temperature, $T = T_r$

in the temperature range of 200-800K. Figure 12 shows the same entropy, at fixed temperature, in the pressure range of 1-10 bar.

A.3 Vapor-liquid equilibrium

The equilibrium matrix K relates the compositions of saturated vapor to the composition of saturated liquid at a given temperature T and pressure P. This relation is written as

$$y = K(T, P)x \tag{50}$$

The relations of vapor and liquid composition is simplified by assuming no component interactions. I.e. the composition of A in the liquid phase does not influence on the composition of P in the vapor phase. This simplification makes K a diagonal matrix. The diagonal elements of K is calculated from the partial pressure of each component and total pressures of the mixture

$$k_{ii} = p_i/P \tag{51}$$

where p_i the partial pressure of component i and P the total pressure. The partial pressure of the components in the mixture is calculated using the Antoine equation

$$p_i = 10^{\left(A_i - \frac{B_i}{T+C_i}\right)} \tag{52}$$

where T is the temperature of the mixture. The Antoine equation parameters is specific for each component and its values was obtained from NIST (2005).

G is not a pure component and the the partial pressure of G set equal to the average partial pressure of the components in G ($(p_{C_2H6}+p_{C_3H8}+p_{C_4H10})/3$).

B Unit models

A unit model describes a small part of the process like a heater, flash drum or compressor. The process model equations of a unit model is organized such that connections between unit models is by process streams. In this modeling framework a process stream is defined as a set of shared variables describing the process stream properties. In this case the process stream variables are selected to be molar component fractions $\boldsymbol{x}$, molar flow F, stream temperature T and stream pressure P.

B.1 Heater

The heater is modeled as a direct heat input to the process stream. The inlet and outlet streams in the vapor phase and no phase changes occurs. The heater has one inlet and one outlet stream as shown in figure 13. The

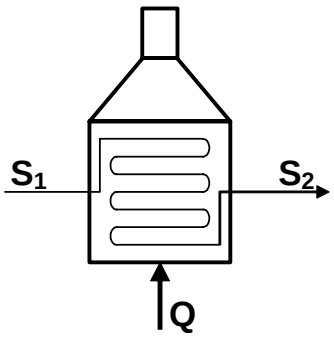

Figure 13: Heater

heater unit model has $n_z = 2(NC + 3) + 1$ variables where $2(NC + 3)$ variables describes the properties of the inlet and outlet streams and one internal variable, the heat input Q. .

The process are the mass balance, energy balance, mole fraction summation and pressure flow relation. The pressure drop is proportional to the squared outlet stream volume flow. The unit model has $n_f = NC + 3$ equations and the degrees of freedom $n_z - n_f = NC + 4$. The equations of the heater unit

model are written as

$$F_1\boldsymbol{x}_1 - F_2\boldsymbol{x}_2 = 0 \tag{53}$$

$$F_1 h_v(\boldsymbol{x}_1, T_1) - F_2 h_v(\boldsymbol{x}_2, T_2) + Q = 0 \tag{54}$$

$$\sum_{i=1}^{NC} \boldsymbol{x}_2(i) - 1 = 0 \tag{55}$$

$$P_2 - P_1 - k_p \left(F_2 \frac{RT_2}{100 P_2} \right)^2 = 0 \tag{56}$$

$$\tag{57}$$

where k_p is a fixed pressure drop constant ([bar/m^3]).

B.2 Reactor (CSTR)

The CSTR unit model is used as a element in the reactor model. This unit model ,as shown in figure 14, has one inlet and one outlet stream which both are in the vapor phase. The unit model has $2(NC+3)$ variables describing the

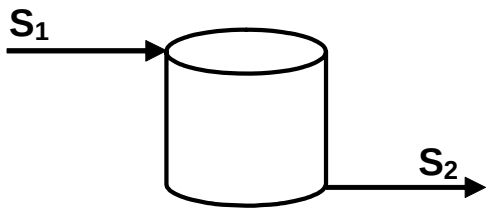

Figure 14: Plug flow reactor element

properties of the inlet and outlet streams and one internal variable, A_c. A_c is a catalyst efficiency factor and has a value close to 1. The unit model total number of variables $n_z = 2(NC + 3) + 1$. The CSTR is modeled by a mass

and energy balance, sum of molar fractions and a pressure-flow equation.

$$F_1\boldsymbol{x}_1 - F_2\boldsymbol{x}_2 + A_c m_c N^{\mathrm{T}} r(T_2, P_2) = 0 \tag{58}$$

$$F_1 h_v(\boldsymbol{x}_1, T_1,) - F_2 h_v(\boldsymbol{x}_2, T_2) + A_c m_c H_r r(T_2, P_2) = 0 \tag{59}$$

$$\sum_{i=1}^{NC} \boldsymbol{x}_2(i) - 1 = 0 \tag{60}$$

$$P_2 - P_1 - kp\left(F_2 \frac{RT_2}{100P_2}\right)^2 = 0 \tag{61}$$

$$\tag{62}$$

where m_c is the mass of catalyst, N the stoichiometric matrix and $r(T, P)$ the reaction rates. H_r is the heat of reaction. The ractor pressure drop is proportional with the squared of the reactor outlet volume flow. The CSTR unit model has $n_f = NC + 3$ equations and the degrees of freedom $n_z - n_f = NC + 4$.

B.3 Separator with water cooling

The cooling water heat exchanger and separator is modeled as one unit model, as shown if figure 15. Feed stream one are in the vapor phase and feed stream two are in the liquid phase. Outlet stream three are in the vapor phase and outlet stream four are in the liquid phase. The heat transfer is modeled as a pure countercurrent heat exchanger where the hot side has liquid and vapor inlet and outlet streams. This unit model has $4(NC + 3)$

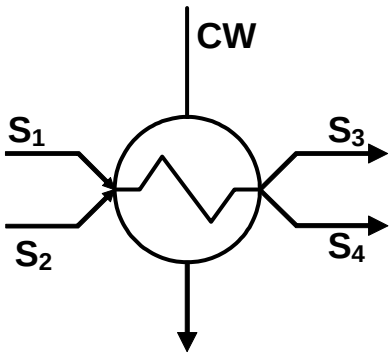

Figure 15: Flash drum

variables describing the properties if the inlet and outlet streams and five internal variables. Tree internal variables describes the cooling water flow,

inlet and outlet temperature and two internal variables are used for heat transfer coefficient U and transferred heat, Q. The total number of model variables $n_z = 4(NC + 3) + 5$

The heat transfer is modeled using the ϵ-Ntu method as described in Mills (1995). There are no pressure drop in the system and the inlet and outlet streams have equal pressures.

The equations of this unit model are the hot side mass balance, hot side energy balance, sum of molar fractions of the hot side liquid and vapor outlet streams, hot side vapor liquid equilibrium, hot side vapor and liquid pressure-flow relation (zero pressure drop), equal temperature in vapor and liquid outlet streams, cold side energy balance (water) and finally a equation describing the heat transfer.

$$F_1\boldsymbol{x}_1 + F_2\boldsymbol{x}_2 - F_3\boldsymbol{x}_3 - F_4\boldsymbol{x}_4 = 0 \quad (63)$$

$$F_1 h_v(\boldsymbol{x}_1, T_1) + F_2 h_l(\boldsymbol{x}_2, T_2) - F_3 h_v(\boldsymbol{x}_3, T_3) - F_4 h_l(\boldsymbol{x}_4, T_3) + Q = 0 \quad (64)$$

$$\sum_{i=1}^{NC} \boldsymbol{x}_3(i) - 1 = 0 \quad (65)$$

$$\sum_{i=1}^{NC} \boldsymbol{x}_4(i) - 1 = 0 \quad (66)$$

$$\boldsymbol{x}_3 - K(T_4, P_4)\boldsymbol{x}_4 = 0 \quad (67)$$

$$P_1 - P_4 = 0 \quad (68)$$

$$P_2 - P_4 = 0 \quad (69)$$

$$T_3 - T_4 = 0 \quad (70)$$

$$F_{CW} Cp_{CW}(T_{CWo} - T_{CWi}) - Q = 0 \quad (71)$$

$$\varepsilon \cdot \mathrm{C_{min}}(T_1 - T_{CWi}) - Q = 0 \quad (72)$$

The subscript CW refers to cooling water where F_{CW}, T_{CWo}, T_{CWi} refers to cooling water flow, outlet and inlet temperature respectively. Fixed specific heat capacity Cp_{CW} is assumed for cooling water.

For a pure countercurrent heat exchanger the efficiency (ε) is defined as

$$\varepsilon = \frac{1 - e^{(-\mathrm{Ntu}(1-\mathrm{R_C}))}}{1 - \mathrm{R_C}\, e^{(-\mathrm{Ntu}(1-\mathrm{R_C}))}} \quad (73)$$

where $\mathrm{R_C}$ is the capacity ratio and Ntu the number of transfer units. $\mathrm{R_C}$ and Ntu are defined as

$$\mathrm{R_C} = \frac{\mathrm{C_{min}}}{\mathrm{C_{max}}} \quad \mathrm{Ntu} = \frac{\mathrm{UA}}{\mathrm{C_{min}}} \quad (74)$$

where U is the heat exchanger heat transfer coefficient and A the heat exchanger area of heat transfer. The minimum and maximum capacity is defined as

$$\mathrm{C_{min}} = \min\left(\mathrm{C_h}, \mathrm{C_c}\right) \quad \mathrm{C_{max}} = \max\left(\mathrm{C_h}, \mathrm{C_c}\right) \tag{75}$$

where $\mathrm{C_h}$ $\mathrm{C_c}$ is the hot and cold side capacity respectively.

$$\mathrm{C_h} = F_h C_{ph} \qquad \mathrm{C_c} = F_c C_{pc} \tag{76}$$

where F_h is the hot side flow and C_{ph} is the hot side specific heat capacity. Similar for the cold side.

The ϵ-Ntu method for calculation of heat transfer is based on hot and cold side fluids with constant specific heat. In this case the hot side fluid is a mixture of vapor and liquid and condensation of vapor occurs. In order to still be able to use this method a approximation of the hot side specific heat is used. We have that the average $C_p = h/\Delta T$. In this case $\bar{h}$ is the average enthalpy of the inlet and outlet of the heat exchanger. The specific enthalpy at the inlet is the weighted average of the liquid and vapor specific enthalpy. The average enthalpy at the inlet and outlet is calculated as

$$\bar{h}_i = \frac{F_1 h_v(\boldsymbol{x}_1, T_1) + F_2 h_l(\boldsymbol{x}_2, T_2)}{F_1 + F_2} \qquad \bar{h}_o = \frac{F_3 h_v(\boldsymbol{x}_3, T_3) + F_4 h_l(\boldsymbol{x}_4, T_4)}{F_3 + F_4} \tag{77}$$

In the reformer model the inlet vapor and liquid stream ar both saturated and are at the same temperature and pressure. The same is also valid for the heat exchanger hot side outlet stream. The average specific heat for the hot side stream is calculated as

$$Cph = \frac{\bar{h}_o - \bar{h}_i}{T_4 - T_2} \tag{78}$$

The separator with cooling unit model has $n_f = 2NC + 8$ equations and has $n_z - n_f = 2NC + 9$ degrees of freedom.

B.4 Compressor

The compressor unit model, as shown in figure 16, has one inlet and one outlet stream. The unit model has $2(NC + 3)$ variables describing the properties of the process streams and tree internal variables. The internal variables are shaft work W, compressor efficiency ψ and isentropic outlet temperature (reversible compression) T_s. The number of variables adds up to $n_z = 2(NC + 3) + 3$. The compressor unit model equations are the mass bal-

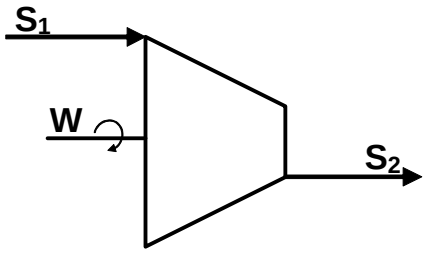

Figure 16: Compressor

ance, energy balance for reversible and irreversible compression, sum of outlet stream mole fractions and reversible compression zero entropy production.

$$F_1\boldsymbol{x}_1 - F_2\boldsymbol{x}_2 = 0 \tag{79}$$

$$F_1 h_v(\boldsymbol{x}_1, T_1) - F_2 h_v(\boldsymbol{x}_2, T_s) + \psi W = 0 \tag{80}$$

$$F_1 h_v(\boldsymbol{x}_1, T_1) - F_2 h_v(\boldsymbol{x}_2, T_2) + W = 0 \tag{81}$$

$$\sum_{i=1}^{NC} \boldsymbol{x}_2(i) - 1 = 0 \tag{82}$$

$$F_1 s_v(\boldsymbol{x}_1, T_1, P_1) - F_2 s_v(\boldsymbol{x}_2, T_s, P_2) = 0 \tag{83}$$

This compressor model model has $n_f = NC + 4$ equations and $n_z - n_f = NC + 5$ degrees of freedom.

B.5 Reactor effluent heat exchanger

The reactor effluent heat exchanger unit model, shown in figure 17, has phase changes in both the hot and the cold side. The cold side inlet stream S_1 is in the vapor phase and S_2 is in the liquid phase. The outlet of the cold side S_3 is in vapor phase.

The hot side feed S_4 is superheated vapor, which is partially condensed into the hot side liquid and vapor outlet streams S_5 and S_6. This model has $6(NC+3)$ variables describing the properties of the hot and cold side inlet and outlet streams. In addition there are two internal variables,heat exchanger duty Q and the heat transfer coefficient U. The total number of variables $n_z = 6(NC + 3) + 2$.

The cold side model is the mass balance, energy balance, sum of outlet stream molar fractions and cold side pressure flow relation (zero pressure drop). The hot side side model is the mass balance, energy balance, sum of outlet streams

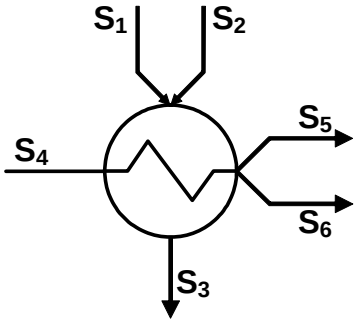

Figure 17: Heat exchanger

molar fractions, vapor-liquid equilibrium and hot side pressure flow relation (zero pressure drop). Finally, the heat transfer is modeled using the ϵ-Ntu method.

$$F_1\boldsymbol{x}_1 + F_2\boldsymbol{x}_2 - F_3\boldsymbol{x}_3 = 0 \tag{84}$$

$$F_1 h_v(\boldsymbol{x}_1, T_1) + F_2 h_l(\boldsymbol{x}_2, T_2) - F_3 h_v(\boldsymbol{x}_3, T_3) + Q = 0 \tag{85}$$

$$\sum_{i=1}^{NC} \boldsymbol{x}_3(i) - 1 = 0 \tag{86}$$

$$P_1 - P_3 = 0 \tag{87}$$

$$P_2 - P_3 = 0 \tag{88}$$

$$F_4\boldsymbol{x}_3 - F_5\boldsymbol{x}_5 - F_6\boldsymbol{x}_6 = 0 \tag{89}$$

$$F_4 h_v(\boldsymbol{x}_4, T_4) - F_5 h_v(\boldsymbol{x}_5, T_5) - F_6 h_l(\boldsymbol{x}_6, T_6) - Q = 0 \tag{90}$$

$$\sum_{i=1}^{NC} \boldsymbol{x}_5(i) - 1 = 0 \tag{91}$$

$$\sum_{i=1}^{NC} \boldsymbol{x}_6(i) - 1 = 0 \tag{92}$$

$$\boldsymbol{x}_5 - K(T_6, P_6)\boldsymbol{x}_6 = 0 \tag{93}$$

$$P_4 - P_5 = 0 \tag{94}$$

$$T_5 - T_6 = 0 \tag{95}$$

$$\varepsilon \cdot \mathrm{C}_{\min}(T_4 - T_1) - Q = 0 \tag{96}$$

The calculation of the heat transfer term in equation 96 is similar to the description in section B.3 equation 73.

This heat exchanger unit model has $n_f = 3NC + 10$ equations and $n_z - n_f =$

$3NC + 10$ degrees of freedom.

B.6 Vapor-liquid stream mixer

This unit model, shown in figure 18, is used to describe the mixing of the liquid feed and recycle gas. There are four process streams in the model, one vapor and one liquid inlet stream, and one vapor and one liquid outlet stream. The inlet steam S_1 and outlet stream S_3 is in the vapor phase and inlet steam

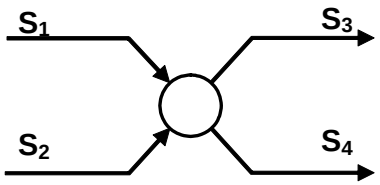

Figure 18: Mixing of vapor and liquid streams

S_2 and outlet stream S_4 in the liquid phase. There are $n_z = 4(NC + 3)$ variables describing the properties of the input and output streams.

The stream mixing model are the mass balance, energy balance, sum of outlet streams molar fractions, vapor-liquid equilibrium and pressure-flow relations (zero pressure drop).

$$F_1\boldsymbol{x}_1 + F_2\boldsymbol{x}_2 - F_3\boldsymbol{x}_3 - F_4\boldsymbol{x}_4 = 0 \tag{97}$$

$$F_1 h_v(\boldsymbol{x}_1, T_1) + F_2 h_l(\boldsymbol{x}_2, T_2) - F_3 h_v(\boldsymbol{x}_3, T_3) - F_4 h_l(\boldsymbol{x}_4, T_4) = 0 \tag{98}$$

$$\sum_{i=1}^{NC} \boldsymbol{x}_3(i) - 1 = 0 \tag{99}$$

$$\sum_{i=1}^{NC} \boldsymbol{x}_4(i) - 1 = 0 \tag{100}$$

$$\boldsymbol{x}_3 - K(T_3, P_3)\boldsymbol{x}_4 = 0 \tag{101}$$

$$P_1 - P_3 = 0 \tag{102}$$

$$P_2 - P_3 = 0 \tag{103}$$

$$T_3 - T_4 = 0 \tag{104}$$

The unit model has $n_f = 2NC + 6$ equations and if the degrees of freedom in this model equals $n_z - n_f = 2NC + 6$.

B.7 Stream split

The stream split unit model, shown in figure describe the split of one vapor stream into two vapor streams. The model has $n_z = 3(NC + 3)$ variables,

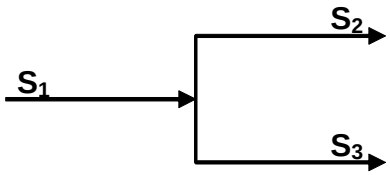

Figure 19: Splitting of streams

describing the properties if the input and output streams.

The stream split model are the mass balance, energy balance, sum of molar fractions, outlet stream equal composition, outlet stream equal temperature, and pressure-flow relations (zero pressure drop).

$$F_1\boldsymbol{x}_1 - F_2\boldsymbol{x}_2 - F_3\boldsymbol{x}_3 = 0 \tag{105}$$

$$F_1 h_v(\boldsymbol{x}_1, T_1) - F_2 h_v(\boldsymbol{x}_2, T_2) - F_3 h_v(\boldsymbol{x}_3, T_3) = 0 \tag{106}$$

$$\sum_{i=1}^{NC} \boldsymbol{x}_3(i) - 1 = 0 \tag{107}$$

$$\boldsymbol{x}_2 - \boldsymbol{x}_3 = 0 \tag{108}$$

$$T_2 - T_3 = 0 \tag{109}$$

$$P_1 - P_2 = 0 \tag{110}$$

$$P_1 - P_3 = 0 \tag{111}$$

The stream split unit model has $n_f = 2NC + 5$ equations and $n_z - n_f = NC + 4$ degrees of freedom.

References

D. Bommannan, R. D. Srivastava, and D. N. Saraf. Modeling of catalytic naphtha reformers. *Canadian journal of chemical engineering*, 67:405–411, 1989.

J. W. Lee, Y. C. Ko, Y. K. Jung, K. S. Lee, and E. S. Yoon. A modeling and simulation study on a naphtha reforming unit with catalyst circulation and regeneration system. *Computers & Chemical Engineering*, 21:S1105–S1110, 1997.

Tore Lid and Sigurd Skogestad. Effective steady state models for simulation, data reconciliation and optimization. *Submitted to Computers & Chemical Engineering*, 2006.

Anthony F. Mills. *HEAT AND MASS TRANSFER*. The Richard D. Irwin series in heat transfer. RICARD D. IRWIN, INC, first edition, 1995.

NIST. *NIST Chemistry WebBook*. National Institute of Standards and Technology, http://webbook.nist.gov/chemistry/, 2005.

R. B. Smith. Kinetic analysis of naphtha reforming with platinum catalyst. *Chemical Engineering Progress*, 55(6):76–80, 1959.

G. M. Stanley and R. S. H. Mah. Observability and redundancy in process data estimation. *Chemical Engineering Science*, 36:259–272, 1981.

Unmesh Taskar and James B. Riggs. Modeling and optimization of a semi-regeneratiove catalytic naphtha reformer. *AIChE Journal*, 43(3):740–753, 1997.

I. B. Tjoa and L. T. Biegler. Simultaneous strategies for data reconciliation and gross error detection of nonlinear systems. *Computers & Chemical Engineering*, 15(10):679–690, 1991.